JOURNAL OF AGRICULTURAL AND FOOD CHEMISTRY

J. Agric. Food Chem. **2006,** *54,* 4611−4616 **4611**

Plasticization of a Protein-Based Film by Glycerol: A Spectroscopic, Mechanical, and Thermal Study

CHUNLI GAO,† MATS STADING,‡ NIKOLAUS WELLNER,† MARY L. PARKER,† TIMOTHY R. NOEL,† E. N. CLARE MILLS,† AND PETER S. BELTON*,§

Institute of Food Research, Colney Lane, Norwich NR4 7UA, United Kingdom, SIK, The Swedish Institute for Food and Biotechnology, P.O. Box 5401, SE-402 29, Göteborg, Sweden, and School of Chemical Sciences and Pharmacy, University of East Anglia, Norwich NR4 7TJ, United Kingdom

Kafirin, the seed storage protein of the cereal sorghum, is highly homologous with the maize storage protein zein. The effects of plasticisation of a kafirin film by glycerol in the absence of water were examined by a combination of spectroscopic (NMR and infrared), rheological, and calorimetric methods. The results suggest that at low glycerol levels the glycerol is absorbed onto and possibly into the protein. Increasing the level of glycerol increases the motion of the protein and changes the protein conformation. There are corresponding changes of the mechanical properties of protein films. At 40% (w/w) of glycerol, two glass transition temperatures were observed, one of which corresponded to the glass transition temperature of pure glycerol. This result indicates that at this level of plasticizer there are sufficient glycerol/glycerol interactions occurring to allow a separate glass formation process for glycerol.

KEYWORDS: Plasticization; glycerol; protein; kafirin; biodegradable; film

INTRODUCTION

There is continuing interest in the production of biodegradable plastics and films based on proteins (*1*), which include a wide range of plant-derived proteins such as soy protein, wheat gluten, and maize zein. Kafirin, the seed storage protein of sorghum, has been very little used as a source of films or coatings (*2*). Sorghum is a major crop in sub-Saharan Africa and is well-suited to the climatic and soil conditions there. Kafirin, while highly homologous to zein, is considerably more hydrophobic and may form a more effective water barrier than other types of protein-based films. In addition to its potential as a film-forming material, kafirin also has the advantage that its use would add value to this important African crop (*3*).

In almost all cases, manufacturing of protein-based films and coatings requires plasticization of the protein in order to improve the flexibility of films and make them easy to handle. Frequently, mixtures of plasticizers are employed; the choice of components and ratios in the mixtures is based on changes in mechanical or permeability parameters of resulting films. While these operational outcomes are the required end point of the process, they do not give any insight into the molecular processes involved in forming films with particular properties. Consequently, our current lack of understanding of interactions between proteins and plasticizers limits our ability to predict the outcome of any particular plasticization regime.

There have been a number of reports on the use of infrared methods to assess molecular changes in plasticized protein systems (*3*−*5*). While they have amply demonstrated the ability of infrared spectroscopy to follow changes in protein conformation, they have typically been carried out in systems where either a number of plasticizer components or water are present. The specific molecular interactions of a single plasticizer and protein are difficult to disentangle from such studies.

While solid state NMR has been used widely to characterize synthetic polymer systems, it has not been well-applied to the study of protein films. Only very recently, cross-polarization and magic angle spinning methods (*7*) have been used to examine a gluten/glycerol/water system and one paper reported transverse relaxation time measurements on soy protein isolate/glycerol/water systems (*8*), in which the distribution of transverse relaxation times and spin lattice relaxation measurements was consistent with the plasticizing effect of water. In this paper, we examine the interaction of only one plasticizer, glycerol, and kafirin using infrared and NMR spectroscopy, thermal methods, and mechanical measurements. In this way, we attempt to build a more complete picture of the changes occurring in the system at the molecular and macroscopic levels. This well-defined system can act as a baseline model for interpretation of more complicated systems to gain insight into mechanisms of plasticization that are more generally applicable.

MATERIALS AND METHODS

Materials. Kafirin was extracted with *tert*-butyl alcohol from a mixture of two condensed tannin-free white sorghum cultivars (PANNAR 202 and 606, ex. B. Koekemoer, Lichtenburg, South Africa, 2001),

* To whom correspondence should be addressed. E-mail: p.belton@uea.ac.uk.
† Institute of Food Research.
‡ The Swedish Institute for Food and Biotechnology.
§ University of East Anglia.

10.1021/jf060611w CCC: $33.50
Published on Web 06/03/2006

using the same method as published previously (*9*). D_8-glycerol was obtained from Cambridge Isotope Laboratories. All other chemicals used were of analytical reagent grade and obtained from Sigma Aldrich (United Kingdom).

Film Casting. Kafirin was weighed into a 25 mL round-bottom flask, and aqueous ethanol (70%, v/v) followed by the plasticizer glycerol were added. Samples were heated to 70 °C and held for 10 min at 70 °C with rapid stirring under condensation. Aliquots of this film mix were weighed into either 5 (1 g of mix) or 9 cm (4 g of mix) diameter plastic Petri dishes and gently swirled to coat the bottom of the dish. The Petri dishes were placed without lids on a level surface (checked with a spirit level) in an oven (without forced draught) at 50 °C overnight. Two replicate films were cast for each film mix. The percentage glycerol added to the film mix is expressed as (weight glycerol × 100)/(weight glycerol + weight kafirin). Typical film thicknesses measured by electronic calipers were 110 μm. For experiments with perdeuterated glycerol films, perdeuterated glycerol was used as the plasticizer. All films were stored in a desiccator over P_2O_5 under vacuum for at least a week until constant weights were obtained; subsequent storage was always over P_2O_5. No evidence of any water signal was found in the IR spectra.

Differential Scanning Calorimetry (DSC). Thermal transitions of the plasticized films were studied by DSC. The films were cut into small strips, and the samples (~10 mg) were weighed into aluminum pans in a dry cabinet, sealed, and scanned together with an empty reference pan using a Perkin-Elmer DSC7 fitted with a liquid nitrogen-controlled cooling accessory. The DSC was calibrated for temperature using the melting of indium (T_m = 156.6 °C) and dodecane (T_m = −9.65 °C) and for heat flow using indium (ΔH = 28.45 J/g). Samples were scanned at 10 °C/min. The inflection point of the heat flow step change, close to the half C_p change of the second heating scan, was taken as the operative definition of the glass transition temperature, T_g.

Film Strength. The film strips (60 mm × 4 mm) were stored dry in a desiccator over P_2O_5 until measurement. A material-testing instrument (Instron 5542, Canton, MA) was used to determine mechanical properties in accordance with ASTM D882-91. The initial grip separation and crosshead speed were set to 40 mm and 24 mm/min, respectively. Force and elongation were recorded during extension, and Young's modulus (E), stress at break (ϵ_b), and strain at break (σ_b) were calculated using the initial gauge length and cross-sectional area of the film strip. Replicates (*5*−*11*) of each experimental point were evaluated.

Thermomechanical Properties. Dynamic mechanical analysis (DMTA) of the films was performed in tension in a Rheometrics RSA-II (Rheometric Scientific, Piscataway, NJ). A rectangular film strip, 4 mm × 30 mm, was clamped in the instrument, and a sinusoidal deformation was applied on top of a static deformation, the sum of these being nondestructive. A recording was made of the resulting force and phase shift, δ to the applied deformation, and the complex tensile modulus, E^*, was calculated. E^* can be divided into the storage modulus (E'), and loss modulus (E''), using the relations $E^* = E' + jE''$, $\tan\delta = E''/E'$, and $j^2 = -1$. The measurements were performed in the temperature interval 30−200 °C using dry air for temperature control. T_g was recorded at the peak in E'' occurring at the glass transition.

All samples were stored in a desiccator over P_2O_5 and quickly (<60 s) inserted in the instrument. The temperature in the DMA furnace was maintained by circulating dry, heated air around the sample. The starting relative humidity was <2% at 20 °C. This decreased at elevated temperatures.

NMR. The films were cut into small strips (10 mm × 2 mm). Solid state NMR spectra and relaxation times were obtained on a Bruker MSL 200 NMR spectrometer operating at 200.13 MHz for ^{1}H. Prior to the ^{1}H relaxation time experiments, the radio frequency pulse amplitudes and phase orthogonality were optimized using a standard multiple pulse tune up procedure. Free induction decays were acquired following a solid echo with ring down delay of 5 μs and a dwell time of 0.5 μs. All curve fitting was carried out using a Levenberg−Marquardt nonlinear curve-fitting routine installed in TableCurve2 2D (Jandel Scientific). For experiments with perdeuterated glycerol, films were equilibrated with D_2O vapor in a jar. The D_2O was changed three times to ensure complete exchange of all exchangeable protons and then stored over P_2O_5 to dry.

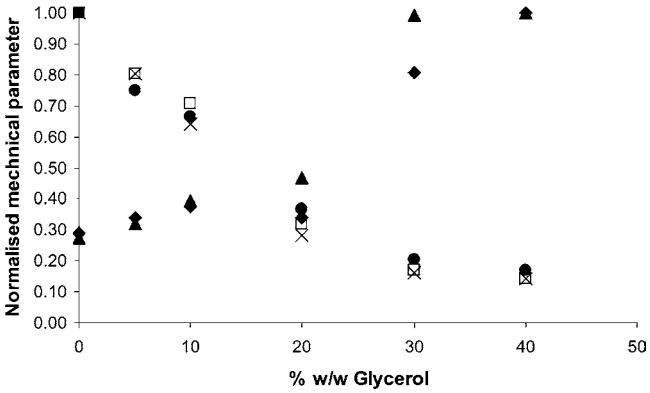

Figure 1. Variation of the normalized mechanical parameters with glycerol content. Strain at maximum stress, ♦; stress at maximum strain, □; strain at break, ▲; stress at break, ×; and Young's modulus, ●.

Table 1. Variation of the Maxima and Minima of the Mechanical Parameters of the Films Cast in the Absence or Presence of 40% (w/w) Glycerol[a]

	glycerol content (% w/w)	
mechanical parameters	0	40
strain at break (%)	2.6 (0.7)	10 (2)
stress at break (MPa)	54 (11)	7.6 (0.4)
stress at max strain (MPa)	54 (11)	7.7 (0.4)
strain at max stress (%)	2.6 (0.7)	9 (2)
Young's modulus (MPa)	2655 (125)	450 (35)

[a] Standard deviations are given in brackets.

Fourier Transform Infrared (FT-IR) Spectroscopy. Spectra of kafirin powder (dried over P_2O_5 in a desiccator under vacuum for a week) and films were obtained on a FTS 175 Spectrometer (Bio-Rad, United Kingdom) using a Golden-Gate Diamond Horizontal Attenuated Total Reflectance sampling device (Specac, United Kingdom). Spectra (256 scans at 2 cm^{-1} resolution) were collected within the frequency range 4000−800 cm^{-1}. The empty crystal was used as background. Fourier self-deconvolution was carried out with the spectrometer software with a K factor of 1.5 and a half width of 15 cm^{-1}. Baseline correction was carried out using the method of Wellner et al. (*10*).

RESULTS AND DISCUSSION

Mechanical Measurements. Mechanical measurements proved to be possible on unplasticized as well as plasticized films. As expected, the results show that the plasticizer had a strong effect on the samples: Stress at maximum strain, strain at maximum stress, stress and strain at break, and Young's modulus all showed a strong dependence on the amount of added plasticizer. As expected, stress and Young's modulus decreased with added plasticizer and strain increased with plasticizer level. Normalized data are shown in **Figure 1**. Maximum and minimum values are shown in **Table 1**.

Glass Transition Temperatures. DMTA and calorimetric measurements of T_g of the films as a function of glycerol content are shown in **Table 2**. In both the mechanical and the calorimetric data, significant changes were present even at the level of 5% (w/w) addition of plasticizer, with good agreement between the data sets. An additional glass transition was seen at −77 °C in the 40% (w/w) glycerol sample by calorimetric measurement (**Figure 2**). This corresponds to the glass transition of glycerol and indicates that at 40% (w/w) of plasticizer, a proportion of the glycerol behaved as a separate phase to the protein with respect to the glass transition. It is also clear that

Table 2. Variation of T_g with Glycerol Content[a]

	glycerol (%, w/w)					
T_g (°C)	0	5	10	20	30	40
calorimetric T_g	145.7	112.2	101.9	86.5	70.9	69.2(–77)
DMTA T_g[b]	154	117	99	73	62	61

[a] The two figures in the last column of the calorimetric data indicate the two transitions found. [b] The DMTA measurements started from room temperature; therefore, no T_g lower than room temperature can be observed.

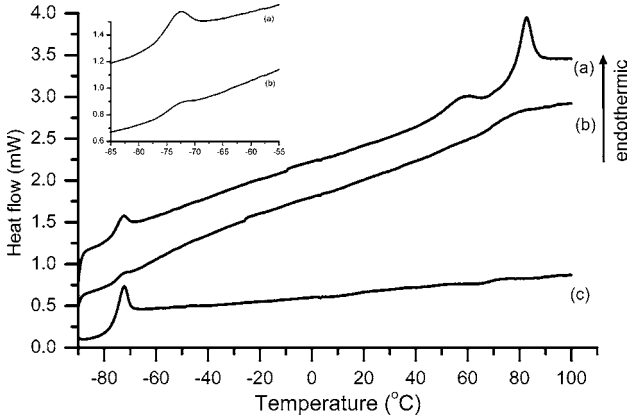

Figure 2. DSC heating scans at 10 K min^{-1} for (**a**) kafarin/40% glycerol, (**b**) immediate rescan of panel **a**, and (**c**) pure glycerol. Traces have been shifted for clarity. The inset shows expansion in the region of glycerol T_g for kafarin/40% glycerol in scans **a** and **b**. The instrument noise level was 0.01 mW.

the high temperature glass transition does not decrease significantly when glycerol content is increased from 30 to 40 % (w/w). The existence of two phase transitions may imply that there are separate phases containing glycerol and protein formed in the 40% sample. The implications of this observation are discussed in the following sections and the general discussion.

The Gordon Taylor equation has previously been used as a means of parametrizing the effects of plasticisation on the glass transition temperatures of cereal proteins (*11*, *12*). It may be written as:

$$T^* = k\frac{W_2}{W_1} \qquad (1)$$

where

$$\left(\frac{T_{g_0} - T_{g_1}}{T_{g_0} - T_{g_2}}\right) = T^*$$

T_{g_0} is the observed T_g, W is the weight fractions, and the subscripts 1 and 2 refer to components 1 and 2, respectively. k is a constant reflecting the plasticizing effect of component 2. A plot of this function for the kafirin/glycerol system is shown in **Figure 3** (the data used were from the calorimetric measurements). It is clear that while the relationship is linear as predicted between 5 and 30% (w/w) glycerol, the value predicted for 40% (w/w) glycerol is low and there are strong deviations between 0 and 5% (w/w) glycerol. These data also indicate that between 30 and 40% (w/w) glycerol, there was a change in the nature of the interaction with the kafirin network, which is supported by the stress and Young's modulus, which also show lower values at 40% (w/w) glycerol than might be expected by the trends of the rest of the curves (**Figure 1**).

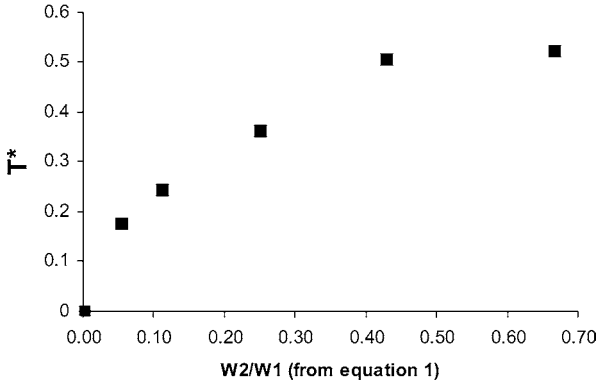

Figure 3. Variation of T^* from eq 1 with the ratio of weight fractions of plasticizer and protein.

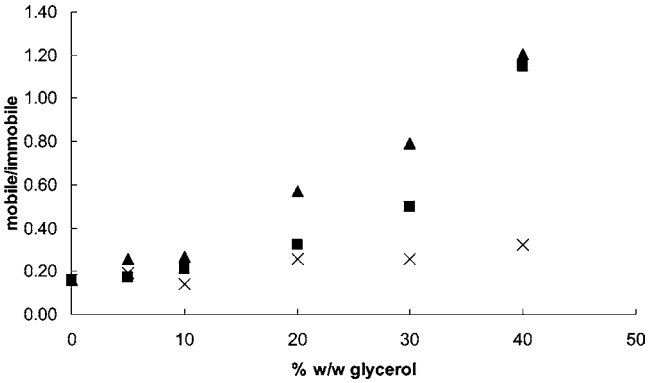

Figure 4. Variation of the ratio of mobile to immobile proton intensities vs glycerol content: protiated glycerol, ■; deuterated glycerol, ×; and the predicted value of the ratio value if glycerol contributes only to the mobile signal, ▲.

NMR Measurements. The proton-free induction decays were fitted to a combination of the Abragam function (*13*) and an exponential as shown in eq 2.

$$M_t = c_1 \exp - \left[\frac{a^2t^2}{2}\right]\left(\frac{\sin bt}{bt}\right) + c_2 \exp - \left[\frac{t}{T_2}\right] \qquad (2)$$

where M_t is the magnetization at time t, a and b are constants, C_i is the intensity arising from component i at $t = 0$, and T_2 is the transverse relaxation time of the exponential component.

The rigid lattice second moment is given by (*13*):

$$M_2 = a^2 + \frac{b^2}{3} \qquad (3)$$

This combination represents the relaxation of a component in the rigid lattice condition (Abragam function) and one in the motional narrowing regime (exponential function). The rigid lattice condition represents a condition in which the frequency of modulation of local dipolar field experienced by the protons is less than the square root of the rigid lattice second moment expressed in frequency units. For typical values for protons, this is of the order of 10^5 s^{-1}. For exponential relaxation, the rates of motion must be faster than this, and for convenience, we therefore refer to motions in the motional narrowing regime as originating from the mobile component and those in the rigid lattice regime as the immobile components. The change in ratio of these components with addition of plasticizer is shown in **Figure 4**.

The data for the protiated glycerol sample show an increasing intensity of the mobile signal with added glycerol. Some of the

mobile component arises from the protein; it is present when there is no added glycerol and increases with the addition of perdeuterated glycerol. Because the resonant nucleus is the hydrogen nucleus, the perdeuterated material does not contribute to the signal. The only signal arising from these samples is from the nonexchangeable protons in the protein. The observation of mobile signal under these circumstances therefore indicates that one effect of the glycerol is to mobilize some of the protein. It seems likely that this mobilization corresponds to the increased motion of the protein side chains at least at the lower glycerol contents. Given the information about the amount of mobilized protein, it is possible to calculate the expected mobile-to-immobile ratio if the glycerol contributes only to the mobile signal. The results of this calculation are shown in **Figure 4**. Large deviations from the observed mobile-to-immobile ratio are only apparent at 20 and 30% (w/w) glycerol. Interpretation of these values must be carried out with care: The calculated ratios involve the manipulation of two sets of data, which are themselves derived from a curve-fitting exercise. The multiplication of errors is therefore considerable. In addition, as the amount of glycerol increases, there is the possibility of exchange between sites, and under these circumstances, the populations of components become a function of the values of the populations, relaxation times, and exchange rates (*14*) and are not indicative of the actual fraction of magnetization relaxing at a particular rate. Given all of these caveats, it would appear to be a reasonable assumption that the glycerol contributes largely to the mobile signal and that in addition it has a role in mobilizing some of the protein network. The behavior of the glycerol is thus consistent with that of synthetic plasticizer in polymer systems (*15*), but it does not offer evidence that the behavior of the 40% (w/w) sample is exceptional. It is interesting to compare these results with those published for the glycerol/gluten system (*7*). In this study, a glycerol signal was observed in the CPMAS spectrum indicating the existence of static dipolar interactions between carbons and protons in the glycerol. In addition to this glycerol, signals were also observed in the single pulse excitation spectrum indicating the existence of glycerol molecules with short spin lattice relaxation times. The latter are normally taken as an indication of the existence of molecules in the motional narrowing region although this is not strictly the case. These results showing a mix of behaviors may well result from the complexity of the material used in the gluten study. The sample contained starch, lipid, water, and some residual fiber as well as protein. The static signal may well therefore arise from interactions with the other components rather than protein and indicate the necessity of working with pure systems before going on to try to interpret the behavior of more complex mixtures.

A plot of the second moment vs glycerol concentration is shown in **Figure 5**. The rigid lattice second moment is a measure of the static dipolar interactions between the protons in the sample. It depends on geometrical factors and the details of the motions undergone by the participating nuclei. In a sample such as the one considered here, both factors may be important. The addition of glycerol changes the conformation of the protein, as shown below, and may cause partial expansion of the protein by solvation. Reduction in the second moment due to motion is also possible. While whole protein rotation at a rate which will reduce the second moment is unlikely in such a concentrated medium, the increase in motion of side chains will reduce the second moment. Other small anisotropic motions induced by solvation will also contribute to the reduction of the second moment.

The general trends and values for both the protiated and the deuterated glycerol samples are the same. However, the scatter

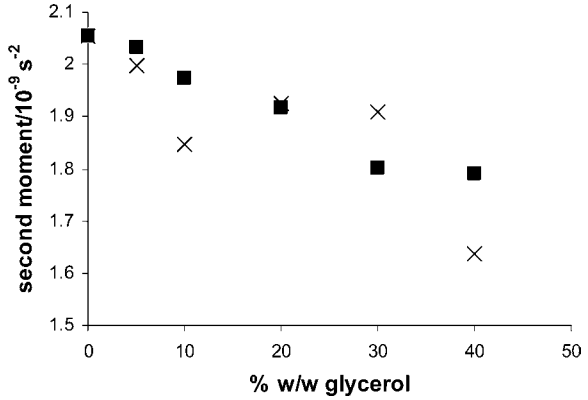

Figure 5. Variation of rigid lattice second moment with glycerol content: protiated glycerol, ■; and deuterated glycerol, ×.

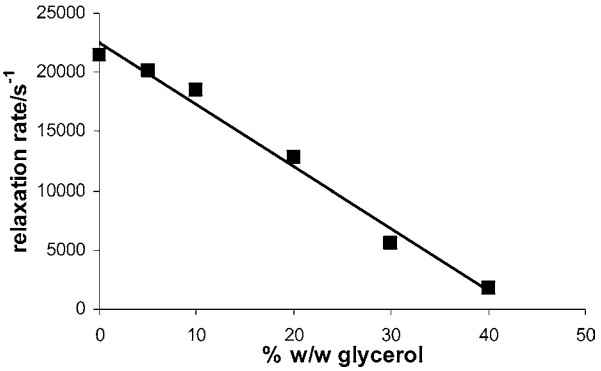

Figure 6. Change in exponential transverse relaxation rate with protiated glycerol content.

in the data from the deuterated samples is much greater than in the protiated data. This is due to due poorer signal-to-noise ratios in the deuterated sample; this particularly effects the estimation of the second moment as in the deuterated data; much of estimation of the "*b*" term depends on data near the baseline. This is not the case for the protiated data, where additional signal from glycerol is present. Within the limitation of scatter, the indication of the trend is that the immobile component arises from the protein only and that glycerol itself does not contribute to the immobile signal. This is consistent with the interpretation of the mobile component relaxation time data. The scatter in the data is such that they do not support an interpretation in which the 40% (w/w) glycerol sample shows little change from the 30% (w/w) glycerol sample even though the protiated data do have experimental values that are similar. The data therefore does not offer any evidence of a phase separation between 30 and 40% (w/w) glycerol; however, it cannot be ruled out on the basis of these data.

The changes in the exponential relaxation rate of the protiated glycerol samples are shown in **Figure 6**, together with a linear fit to the data. The fit is good ($r^2 = 0.9855$) and is consistent with relaxation of the glycerol being driven by fast exchange with exchangeable fast relaxing protein protons (*14*). The 40% (w/w) glycerol sample fits into the trend well and as such does not indicate anomalous behavior, which might be expected if the glycerol were in a separate phase at this concentration. However, even if there were a separate glycerol phase, it may not appear as a separate NMR visible entity in these experiments if exchange between the glycerol-rich phase and the protein-rich phase were fast enough. In systems such as these, the criterion for fast exchange is that (*14*):

$$2\sqrt{2}(A^2/\pi^2 D)|\Delta\gamma| > 1$$

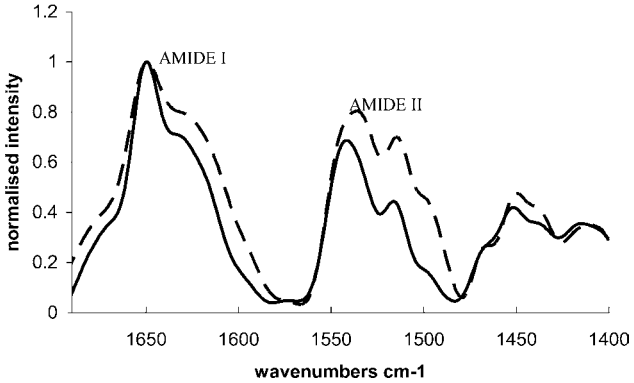

Figure 7. Infrared spectra of samples containing 0 (light line) and 40% (w/w) (heavy line) glycerol; the spectra have been Fourier self-deconvoluted. For ease of comparison, intensities are normalized so that in both spectra the intensity at 1650 cm^{-1} is 1.

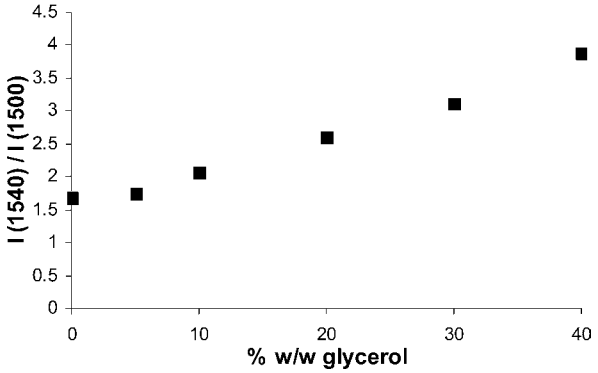

Figure 8. Ratio of the intensities at 1540 to 1500 cm^{-1} in the amide II band of the infrared spectra as a function of glycerol content.

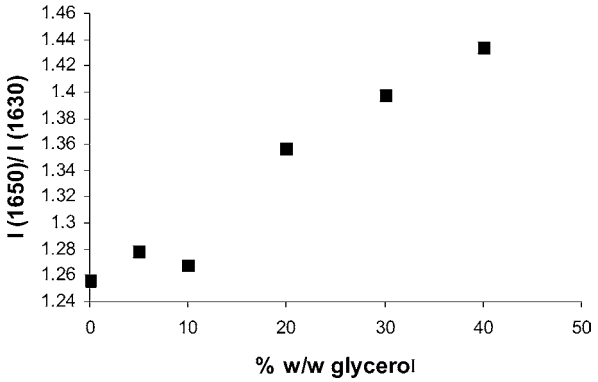

Figure 9. Ratio of the 1650 to 1630 cm^{-1} intensities in the amide I band of the infrared spectra as a function of plasticizer content.

where A is the dimension characterizing the distance over which exchange takes place, D is the diffusion coefficient of the exchanging entity, and $\Delta\gamma$ is the difference in relaxation rates. $\Delta\gamma$ may be estimated conservatively by assuming that the protein phase has a relaxation rate similar to that of the 30% system (i.e., the highest glycerol concentration at which there is definitely not two phases) and the rate for the glycerol phase similar to that from the 40% sample. This gives a value of about 4000 s^{-1}. D will scale with the viscosity of the glycerol and be about 3 orders of magnitude less than that for water and thus take a value of about 1×10^{-12} m^2 s^{-1}. These figures suggest a distance scale of about 30 nm for the characteristic dimension of the glycerol phase and are an upper limit of size. Even though light micrographs showed some inhomogeneity of the plasticized films as compared to homogeneous nonplasticized film (graphs not shown), the resolution of the micrographs is insufficient to offer any evidence in support, but if a separate glycerol phase does exist, it must be present on a very small length scale.

FT-IR. The infrared spectra of films with 0 and 40% (w/w) glycerol are compared in **Figure 7**. There were significant differences in the amide I and II regions between the unplasticized and the plasticized samples. The relative intensities of the peaks contained in both the amide I and the amide II bands change, and the width of both of these bands also changes. In the unplasticized material, the bands are much broader than in the fully plasticized material. This may be taken as an indication that the distribution of protein conformations changes with increasing plasticizer content. The amide II band arises from vibrations, which are mainly due to N−H bending (*16*), and is therefore sensitive to hydrogen bonding, with stronger hydrogen-bonded peptide groups absorbing at higher frequency. In **Figure 8**, the ratio of intensities of the 1540 cm^{-1} peak to the 1500 cm^{-1} peak as a function of glycerol content is plotted. It shows that as the plasticizer level increases, so does the relative intensity of the component at 1540 cm^{-1}. This may be due to two main factors: first, more extensive hydrogen bonding between the protein backbone and the glycerol will reduce the number of nonbonded peptide groups; hence, more hydrogen-bonded peptide groups in the protein will result in a shift to higher frequency thus reducing intensity in the low-frequency region; second, there is a shift from β-sheet structure, which absorbs around 1525 cm^{-1}, to α-helical structure, which has its amide II maximum at 1545 cm^{-1}.

The amide I band can be used to gauge the proportions of different types of protein secondary structure. The positions of the maximum at 1650 cm^{-1} and the shoulder at 1630 cm^{-1} do not change significantly over the whole range of glycerol contents. However, **Figure 9** showed that with an increasing amount of plasticizer the intensity at 1650 cm^{-1} increased at the expense of the intensity at 1630 cm^{-1}. The region around 1650 cm^{-1} may be assigned to contributions from α-helical and disordered conformations (*17*−*19*). The details of the assignment of the 1630 cm^{-1} are not straightforward. Generally, β-sheets absorb in the range of 1610−1635 cm^{-1}. Often, the low-frequency range is assigned to intramolecular interactions and hydrated extended turns and the higher range is assigned to intermolecular interactions (*16*, *17*), although the picture may be more complex (*16*). Whatever the exact assignment, it is clear that plasticizer reduces the amount of this component. It should be noted that, although there is an apparent slight anomaly of behavior in the 10% (w/w) glycerol sample in the amide I region, in general, the changes in the amide I and II regions are smooth across the whole range of the concentration of glycerol and there is no abrupt change between 30 and 40% (w/w) glycerol. Published spectra of kafirin (*9*, *18*) have shown that kafirin dissolved in ethanol or fully hydrated has a high level of α-helical structure, whereas dry proteins or films largely comprise the intermolecular β-sheet, suggesting that the protein secondary structure changes on solvation. Thus, in summary, the infrared data may be interpreted that increasing the glycerol content increases the amount of α-helical and disordered conformations at the expense of β-sheet conformations (*18*, *19*). This seems to be consistent with the NMR data but contrary to the DSC and mechanical data. This is discussed further in the next section.

DISCUSSION

The changes in secondary structure observed by the infrared spectroscopy can be related to the increased mobility of the

protein observed by NMR. The rigid dry protein has many intermolecular protein/protein interactions that contribute to the intensity in the 1630 cm^{-1} region. As the glycerol content increases, these interactions are reduced and the interacting regions either adopt an α-helical structure or form solvated loops. The net effect of this is to increase mobility by increasing the distance between proteins, thus allowing a general increase in motion, as discussed in the section on NMR.

The NMR data suggest that, while there is a consistent pattern of glycerol−protein interaction, as evidenced by the decrease in second moment, glycerol only contributes to the signal from the mobile fraction. There is no evidence from either NMR or infrared spectroscopy of anomalous behavior at the 40% (w/w) glycerol level consistent with the formation of a separate phase of glycerol. In contrast, the changes in some of the mechanical properties of the system are consistent with a change in behavior at the 40% level and might arise from a phase separation, since in such a system the presence of small liquidlike inclusions would be expected to change the nature of the mechanical properties. We have also noticed that in handling the 40% (w/w) glycerol films there is a tendency for glycerol to leach out supporting the notion that a separate glycerol phase is formed.

A possible explanation of these results lies in the consideration of the processes that are occurring at the molecular level. At low glycerol levels, the glycerol is absorbed onto and possibly into the protein in a manner analogous to the way individual water molecules may bind to specific parts of a protein's structure and can even be termed "structural water". This increases motion and affects the protein conformation allowing the adoption a secondary structure associated with the solvated protein. At low levels of glycerol, most of the interactions that are occurring between molecules are either protein−protein interactions or protein−glycerol interactions. There are relatively few glycerol−glycerol interactions. As the amount of glycerol increases, the number of glycerol−glycerol interactions increases. At some point between 30 and 40% w/w glycerol, the number of these interactions is sufficient that at least some of the glycerol has properties similar to that in a bulk phase, and this can undergo a glass transition. Because the proteins are still diluted by the glycerol, at this point, there are continuing reductions in protein−protein interactions, which affect the FTIR and NMR behavior. However, the nature of the plasticization has changed from a situation in which plasticization behavior is dominated by glycerol−protein interactions to one in which glycerol−glycerol interactions play a significant role. Thus, there is a change in the trend of mechanical behavior.

The process of plasticisation of kafirin films by glycerol may be a model for the behavior of this plasticizer in many other systems. The combination of spectroscopic, mechanical, and calorimetric studies on the same system offers a route to a greater understanding of plasticized protein films.

ACKNOWLEDGMENT

We thank Nigel Clayden for help with the NMR and access to his equipment.

LITERATURE CITED

(1) Gennadios, A., Ed. *Protein Based Films and Coatings*; CRC Press: Boca Raton, 2002.
(2) Buffo, R. A.; Weller, C. L.; Gennadios, A. Films from laboratory extracted kafirin. *Cereal Chem.* **1997**, *74*, 473−475.
(3) Belton, P. S.; Taylor, J. R. N. Sorghum and millets: protein sources for Africa. *Trends Food Sci. Technol.* **2004**, *15*, 94−98.
(4) Guegen, J.; Viroben, G.; Noireaux, P.; Subirade, M. Influence of plasticizers and treatment on the properties of films from various pea proteins. *Ind. Crop Prod.* **1998**, *7*, 149−157
(5) Subirade, M.; Kelly, I.; Guegen, J.; Pezolet, M. Molecular basis of film formation from a soybean protein: Comparison between the conformation of glycinin in aqueous solution and in films. *Int. J. Biol. Macromol.* **1998**, *23*, 241−249.
(6) Mangavel, C.; Barbot, J.; Popineau, Y.; Guegen, J. Evolution of wheat gliadins conformation during film formation: A Fourier transform infrared study. *J. Agric. Food Chem*. **2001**, *49*, 867−872.
(7) Zhang, X.; Burger, I.; Do, M. D.; Lourbakis, E. Intermolecular interactions and phase structures of plasticized wheat protein films. *Biomacromolecules* **2005**, *6*, 1661−1671.
(8) Choi, S.-G.; Kim, M. A.; Weller, C. L.; Kerr, W. L. Molecular dynamics of soy-protein isolate films plasticized by water and glycerol. *J. Food Sci*. **2003**, *68*, 2516−2522.
(9) Gao, C.; Taylor, J. R. N.; Wellner, N.; Byaruhanga, Y. B.; Parker, M. L.; Mills, E. N. C.; Belton, P. S. Effect of preparation conditions on protein secondary structure and biofilm formation of kafirin. *J. Agric. Food Chem.* **2005**, *53*, 306−312.
(10) Wellner, N.; Mills, E. N. C.; Brownsey, G.; Wilson, R. H.; Brown, N.; Freeman, J.; Halford, N. G.; Shewry, P. R.; Belton, P. S. Changes in protein secondary structure during gluten deformation studied by dynamic Fourier transform infrared spectroscopy. *Biomacromolecules* **2005**, *6*, 255−261.
(11) Micard, V.; Guilbert, S. Thermal behaviour of native and hydrophobized wheat gluten, gliadin and glutenin rich fractions by modulated DSC. *Int. J. Biol. Macromol.* **2000**, *27*, 229−236.
(12) Barreto, P. L. M.; Roeder, J.; Crespo, J. S.; Maciel, G. R.; Terenzi, H.; Pires, A. T. N.; Soldi, V. Effect of concentration, temperature and plasticizer content rheological properties of sodium caseinate and sodium caseinate/sorbitol solutions and glass transitions of their films. *Food Chem.* **2003**, *82*, 425−431.
(13) Abragam, A. *The Principles of Nuclear Magnetism*; Oxford University Press: Oxford, 1978; p 120.
(14) Belton, P. S. NMR studies of protein hydration. *Prog. Biophys. Mol. Biol*. **1994**, *61*, 61−79.
(15) McBrierty, V. J.; Packer, K. J. *Nuclear Magnetic Resonance in Polymers*; Cambridge University Press: Cambridge, 1993; p 234.
(16) Jung, C. Insight into protein structure and protein−ligand recognition by Fourier transform infrared spectroscopy. *J. Mol. Recognit.* **2000**, *13*, 325−351.
(17) Arrondo, J. L. R.; Goni, F. M. Structure and dynamics of membrane proteins as studied by infrared spectroscopy. *Prog. Biophys. Mol. Biol.* **1999**, *72*, 367−405.
(18) Duodu, K. G.; Tang, H.; Grant, A.; Wellner, N.; Belton, P. S.; Taylor, J. R. N. FTIR and solid-state NMR spectroscopy of proteins of wet cooked and popped sorghum and maize. *J. Cereal Sci.* **2001**, *33*, 261−269.
(19) Feeney, K. A.; Wellner, N.; Gilbert, S. M.; Halford, N. G.; Tatham, A. S.; Shewry, P. R.; Belton, P. S. Molecular structures and interactions of repetitive peptides based on wheat glutenin subunits depend on chain length. *Biopolymers* **2003**, *72*, 123−131.

Received for review March 2, 2006. Revised manuscript received April 25, 2006. Accepted May 4, 2006. Funding is gratefully acknowledged from the EU ENVIROPAK project (ICA4-CT-2001-10062) and from the BBSRC's core strategic grant to IFR.

JF060611W